

University of Wollongong Research Online

Australian Institute for Innovative Materials -
Papers

Australian Institute for Innovative Materials

1-1-2012

The magnetic structure of an epitaxial BiMn_{0.5}Fe_{0.5}O₃ thin film on SrTiO₃ (001) studied with neutron diffraction

David Laurence Cortie

University of Wollongong, dlc422@uowmail.edu.au

A PJ Stampfl

The Institute for Superconducting and Electronic Materials (ANSTO)

F Klose

The Institute for Superconducting and Electronic Materials (ANSTO), Frank.Klose@ansto.gov.au

Y Du

University of Wollongong, ydu@uow.edu.au

Xiaolin Wang

University of Wollongong, xiaolin@uow.edu.au

See next page for additional authors

Follow this and additional works at: <https://ro.uow.edu.au/aiimpapers>



Part of the [Engineering Commons](#), and the [Physical Sciences and Mathematics Commons](#)

Recommended Citation

Cortie, David Laurence; Stampfl, A PJ; Klose, F; Du, Y; Wang, Xiaolin; Zhao, H; Kimura, H; and Cheng, Z, "The magnetic structure of an epitaxial BiMn_{0.5}Fe_{0.5}O₃ thin film on SrTiO₃ (001) studied with neutron diffraction" (2012). *Australian Institute for Innovative Materials - Papers*. 570.
<https://ro.uow.edu.au/aiimpapers/570>

Research Online is the open access institutional repository for the University of Wollongong. For further information contact the UOW Library: research-pubs@uow.edu.au

The magnetic structure of an epitaxial BiMn_{0.5}Fe_{0.5}O₃ thin film on SrTiO₃ (001) studied with neutron diffraction

Abstract

High-angle neutron diffraction was used to directly reveal the atomic-scale magnetic structure of a single-crystalline BiMn_{0.5}Fe_{0.5}O₃ thin film deposited on a SrTiO₃ (001) substrate. The BiMn_{0.5}Fe_{0.5}O₃ phase exhibits distinctive magnetic properties that differentiate it from both parent compounds: BiFeO₃ and BiMnO₃. A transition to long-range G-type antiferromagnetism was observed below 120 K with a (1 2 1 2) propagation vector. A weak ferromagnetic behavior was measured at low temperature by superconducting quantum interference device (SQUID) magnetometry. There is no indication of the spin cycloid, known for BiFeO₃, in the BiMn_{0.5}Fe_{0.5}O₃ thin film. The neutron diffraction suggests a random distribution of Mn and Fe over perovskite B sites. 2012 American Institute of Physics.

Keywords

epitaxial, 3, structure, thin, magnetic, film, srtio, 001, studied, neutron, diffraction, 5o, 5fe, bimn

Disciplines

Engineering | Physical Sciences and Mathematics

Publication Details

Cortie, D. L., Stampfl, A. P.J., Klose, F., Du, Y., Wang, X., Zhao, H., Kimura, H. & Cheng, Z. (2012). The magnetic structure of an epitaxial BiMn_{0.5}Fe_{0.5}O₃ thin film on SrTiO₃ (001) studied with neutron diffraction. *Applied Physics Letters*, 101 (17), 1-4.

Authors

David Laurence Cortie, A P.J. Stampfl, F Klose, Y Du, Xiaolin Wang, H Zhao, H Kimura, and Z Cheng

The magnetic structure of an epitaxial BiMn_{0.5}Fe_{0.5}O₃ thin film on SrTiO₃ (001) studied with neutron diffraction

D. L. Cortie, A. P. J. Stampfl, F. Klose, Y. Du, X. L. Wang et al.

Citation: *Appl. Phys. Lett.* **101**, 172404 (2012); doi: 10.1063/1.4762818

View online: <http://dx.doi.org/10.1063/1.4762818>

View Table of Contents: <http://apl.aip.org/resource/1/APPLAB/v101/i17>

Published by the [American Institute of Physics](#).

Related Articles

Structures and magnetism of multinuclear vanadium-pentacene sandwich clusters and their 1D molecular wires
J. Chem. Phys. **137**, 164309 (2012)

Mechanisms of magnetization reversal in stadium-shaped particles
J. Appl. Phys. **112**, 083906 (2012)

Equilibrium magnetic states in individual hemispherical permalloy caps
Appl. Phys. Lett. **101**, 132419 (2012)

Electronic and magnetic structure of Fe₃O₄/BiFeO₃ multiferroic superlattices: First principles calculations
J. Appl. Phys. **112**, 063925 (2012)

Thermalized ground state of artificial kagome spin ice building blocks
Appl. Phys. Lett. **101**, 112404 (2012)

Additional information on *Appl. Phys. Lett.*

Journal Homepage: <http://apl.aip.org/>

Journal Information: http://apl.aip.org/about/about_the_journal

Top downloads: http://apl.aip.org/features/most_downloaded

Information for Authors: <http://apl.aip.org/authors>

ADVERTISEMENT



Goodfellow
metals • ceramics • polymers • composites
70,000 products
450 different materials
small quantities fast

www.goodfellowusa.com

The magnetic structure of an epitaxial $\text{BiMn}_{0.5}\text{Fe}_{0.5}\text{O}_3$ thin film on SrTiO_3 (001) studied with neutron diffraction

D. L. Cortie,^{1,2,a)} A. P. J. Stampfl,² F. Klose,² Y. Du,¹ X. L. Wang,¹ H. Y. Zhao,³ H. Kimura,³ and Z. X. Cheng¹

¹*The Institute for Superconducting and Electronic Materials, The University of Wollongong, Wollongong, NSW 2522, Australia*

²*Australian Nuclear Science and Technology Organisation, Lucas Heights, NSW 2234, Australia*

³*National Institute for Materials Science, Sengen 1-2-1, Tsukuba 305-0047, Japan*

(Received 28 June 2012; accepted 8 October 2012; published online 25 October 2012)

High-angle neutron diffraction was used to directly reveal the atomic-scale magnetic structure of a single-crystalline $\text{BiMn}_{0.5}\text{Fe}_{0.5}\text{O}_3$ thin film deposited on a SrTiO_3 (001) substrate. The $\text{BiMn}_{0.5}\text{Fe}_{0.5}\text{O}_3$ phase exhibits distinctive magnetic properties that differentiate it from both parent compounds: BiFeO_3 and BiMnO_3 . A transition to long-range G-type antiferromagnetism was observed below 120 K with a $(\frac{1}{2}\frac{1}{2}\frac{1}{2})$ propagation vector. A weak ferromagnetic behavior was measured at low temperature by superconducting quantum interference device (SQUID) magnetometry. There is no indication of the spin cycloid, known for BiFeO_3 , in the $\text{BiMn}_{0.5}\text{Fe}_{0.5}\text{O}_3$ thin film. The neutron diffraction suggests a random distribution of Mn and Fe over perovskite B sites. © 2012 American Institute of Physics.

<http://dx.doi.org/10.1063/1.4762818>

The co-existence of magnetic and ferroelectric order in multiferroic materials offers an enticing range of applications which has given impetus to widespread research.^{1–6} The capability to control magnetization using an electric field, via the magnetoelectric effect, provides a promising approach for designing devices that exploit both electronic charge and spin.^{3,5,6} Two materials have emerged as prominent candidates for such applications: BiFeO_3 ^{2,3} and BiMnO_3 .^{5,7} The widespread interest in BiFeO_3 originates because it possesses stable ferroelectric and antiferromagnetic order at room temperature⁸ ($T_N = 643$ K). However, pure BiFeO_3 has a low magnetic moment in bulk and thin film form,^{2,5} owing to the formation of an incommensurate spin cycloid that minimizes coherent spin canting (weak ferromagnetism).^{9,10} To date, BiMnO_3 is the only material where the coexistence of true ferromagnetic and ferroelectric order has been reported,^{5,7,11,12} albeit with a low magnetic ordering temperature (≈ 100 K). To complicate matters, it appears that ferromagnetic and antiferromagnetic exchange interactions compete in BiMnO_3 , and the resulting ground state depends on applied pressure.¹³ Second, variable oxygen stoichiometry can affect the crystal and magnetic structure.¹²

Study of the $\text{BiMn}_x\text{Fe}_{1-x}\text{O}_3$ series provides a unique pathway towards producing an optimized multiferroic. The substitution of Fe by Mn to form $\text{BiMn}_x\text{Fe}_{1-x}\text{O}_3$ is well-known to lead to an increase in magnetic moment and a decrease in magnetic ordering temperature with x .^{14–17} Sosnowska *et al.* studied the magnetic structure of bulk $\text{BiMn}_x\text{Fe}_{1-x}\text{O}_3$ with $x = 0.0$ – 0.2 using neutron diffraction and reported a G-type antiferromagnetic spin structure with a reduced Néel temperature (560 K), and a systematic suppression of the incommensurate spin cycloid with the addition of Mn.¹⁶ Bulk studies of the $\text{BiMn}_x\text{Fe}_{1-x}\text{O}_3$ series have usually been confined to lower Mn concentrations ($x < 0.3$).^{14,15}

Definitive data on the magnetic structure of bulk $\text{BiMn}_{0.5}\text{Fe}_{0.5}\text{O}_3$ are not yet available because phases containing high Mn concentration are metastable, and single phase powders cannot be fabricated¹⁸ unless high pressures are employed.^{11,19} One approach to overcome this problem has been to co-dope large amounts (10%–50% per atom) of lanthanum.^{17,20} A recently published study reported G-type antiferromagnetic order for bulk $\text{La}_y\text{Bi}_{1-y}\text{Mn}_{0.5}\text{Fe}_{0.5}\text{O}_3$ although the addition of La influenced the crystalline and magnetic properties.²¹ In thin film form, high Mn concentration $\text{BiMn}_{0.5}\text{Fe}_{0.5}\text{O}_3$ can be stabilized without the addition of La due to epitaxial matching on SrTiO_3 ,^{17,22–25} or unconventional low-temperature deposition on Si,²⁶ but experimental results differ. From a theoretical perspective, first-principles calculations for $x = 0.5$ predict a mixture of antiferromagnetic and ferromagnetic superexchange bonds, with antiferromagnetic exchange dominating overall.^{25,27} This could either lead to a ferrimagnetic ($1 \mu_B$ per Fe/Mn atomic pair) or a canted/uncanted antiferromagnetic ground state ($\approx 0 - 0.2 \mu_B$ per Fe/Mn pair) depending on the manner in which Fe and Mn arrange on perovskite B sites.^{25,27} Structural data to clarify this point are lacking because previous x-ray investigations could not distinguish Fe and Mn site ordering due to the similar scattering form factors of the two elements. Neutron diffraction can resolve Fe/Mn site preference and magnetic order on atomic scales but so far no such data have been published for this important compound. Here, the first neutron diffraction study of a $\text{BiMn}_{0.5}\text{Fe}_{0.5}\text{O}_3$ epitaxial thin film is reported.

In this work, polycrystalline Bi:Fe:Mn:O 2:1:1:6 targets were synthesized by a conventional solid-state method. $\text{BiMn}_{0.5}\text{Fe}_{0.5}\text{O}_3$ films were deposited on (001)-cut SrTiO_3 (STO) substrates using pulse-laser deposition at 650 °C with $\approx 500 - 600$ mTorr oxygen pressure.²² X-ray diffraction was conducted on an X'Pert Panalytical Pro lab source using Cu-K α radiation ($\lambda = 1.54$ Å). Neutron diffraction was conducted by operating the TAIPAN Triple-Axis spectrometer,

^{a)}Electronic mail: dcr@ansto.gov.au.

based at the OPAL research reactor in Sydney, in elastic mode at a wavelength of $\lambda = 2.34$ Å. A PG filter was placed before and after the sample to suppress higher-order wavelengths. A Quantum Design 5 T MPMS was used for SQUID magnetometry measurements.

Fig. 1(a) is the x-ray diffraction pattern obtained in standard Bragg-Brentano geometry at 300 K, plotted as a function of $Q_z = \frac{4\pi \sin(\theta)}{\lambda}$ to allow direct comparison with the neutron result. In this work, the (001) direction is taken to be the out-of-plane direction for the film; the (110) and (100) directions correspond to cubic in-plane directions. Strong reflections are seen for the film near the (00n) reflections of the STO(001) substrate. These are indexed using the pseudo-cubic notation. The film has an out-of-plane lattice constant of 4.01 Å. By a linear extrapolation of the lattice constant trend from lower Mn concentrations ($x = 0, 0.1, 0.2$) in the bulk $\text{BiMn}_x\text{Fe}_{1-x}\text{O}_3$ series,¹⁶ in accordance with Vegard's empirical rule, the rough prediction for the pseudo-cubic lattice constant of $\text{BiMn}_{0.5}\text{Fe}_{0.5}\text{O}_3$ is $a = \frac{a_p}{\sqrt{2}} = 3.93$ Å, which agrees well with existing experimental data for the in-plane lattice constant.²⁴ This in-plane constant of $\text{BiMn}_{0.5}\text{Fe}_{0.5}\text{O}_3$ leads to a strain of only 0.6% with the SrTiO_3 ($a = 3.905$ Å). If in-plane lattice matching causes out-of-plane expansion in order to conserve unit cell volume, as is the case for BiFeO_3 thin films,² the out-of-plane lattice constant should be increased to 3.99 Å for $\text{BiMn}_{0.5}\text{Fe}_{0.5}\text{O}_3$ on SrTiO_3 (100), close to what is observed experimentally. The rocking-curves for the (002) film peak were found to be sharp with full-width at half maximum of $\approx 0.13^\circ$. The smaller peak below 001 reflection marked * is a spectral line from tungsten.

Fig. 1(b) is the neutron diffraction pattern at room temperature for the same out-of-plane scattering-vector direction. The (002) peak of the film is resolvable within the instrument resolution as a shoulder on the substrate (002) peak, giving an identical lattice constant to the x-ray result. However, given the structural model, the (001) neutron peak is expected to be weaker because of the different form factors involved for O,

Fe, and Mn. The ratio of neutron Bragg intensity at (002) to the (001) depends on the Mn concentration so that to first approximation $\frac{I(002)}{I(001)} \propto 160e^{-8.19x}$ (1.9 for $x = 0.5$). Thus, the diffraction results imply that Mn is predominantly incorporated into the B site of the $\text{BiMn}_{0.5}\text{Fe}_{0.5}\text{O}_3$ phase, since widespread segregation of Mn rich phases should either lead to a significantly stronger (001) neutron reflection or secondary-phase Bragg reflections. Energy-dispersive x-ray mapping (EDS) on the same sample reveals that the Bi:Fe:Mn ratio is homogeneous over a 1 μm region with a ratio of 2:0.52:0.49. Cross-sectional electron microscopy found the film to be 5900 Å thick. No distinct thin film peaks were observed in the neutron diffraction when the sample was rotated to orientate the scattering vector to the in-plane direction, suggesting that the film and SrTiO_3 share an in-plane lattice constant that is too similar to differentiate within instrumental resolution.

Fig. 2(a) shows the appearance of the $(\frac{1}{2}\frac{1}{2}\frac{1}{2})$ neutron Bragg reflection at low temperature in zero applied field. This peak implies a doubling in the real-space periodicity of the unit cell, corresponding to a transition to antiferromagnetic order. The observed combination of low transition temperature with antiferromagnetic order differentiates the $\text{BiMn}_{0.5}\text{Fe}_{0.5}\text{O}_3$ phase from both parent phases BiFeO_3 and BiMnO_3 , demonstrating that the additional Fe-O-Mn exchange interaction dramatically alters the overall magnetic behavior. Fig. 2(b) is the intensity of the antiferromagnetic peak as a function of temperature after zero-field-cooling. The disappearance of this $(\frac{1}{2}\frac{1}{2}\frac{1}{2})$ peak at temperatures > 120 K implies a magnetic origin. Site preference of Fe and Mn could lead to a similar feature, but in that case a residual peak should remain at higher temperatures, and higher-order reflections should be apparent. Indeed, no strong superlattice peaks could be detected at room temperature at the $(\frac{1}{2}00)$, $(\frac{1}{2}\frac{1}{2}0)$, or $(\frac{1}{2}0\frac{1}{2})$ positions, suggesting that Mn and Fe are randomly disordered across B sites within the host perovskite.

Fig. 2(c) is the net magnetic moment of the sample measured by SQUID magnetometry, upon heating from 10 K in a measurement field of 0.05 T after first cooling from

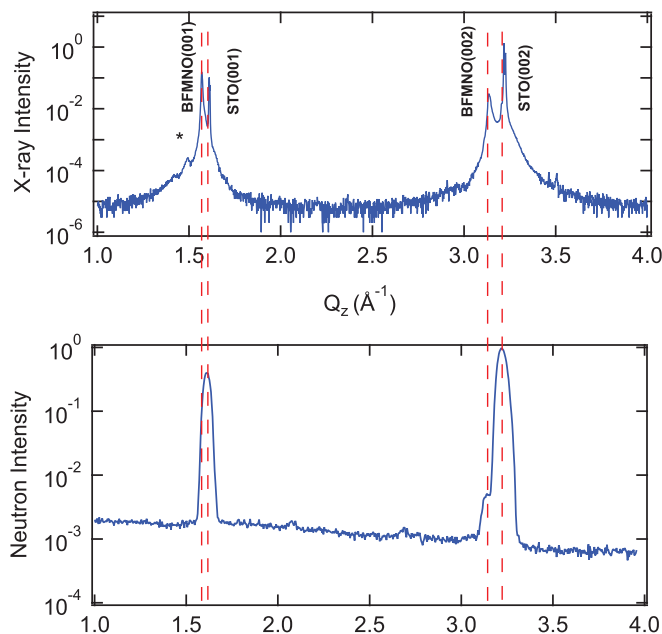


FIG. 1. (a) X-ray ($\lambda = 1.54$ Å) and (b) neutron diffraction of film ($\lambda = 2.34$ Å) with the scattering vector orientated parallel to the 00L direction.

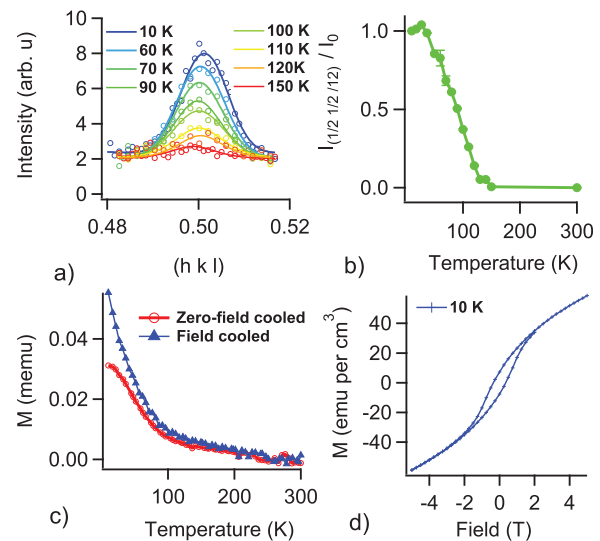


FIG. 2. (a) Neutron diffraction scans of the $(\frac{1}{2}\frac{1}{2}\frac{1}{2})$ Bragg reflection at different temperatures. (b) Integrated intensity of the $(\frac{1}{2}\frac{1}{2}\frac{1}{2})$ Bragg peak as function of temperature. (c) Magnetic moment as function of temperature measured with SQUID magnetometry. (d) In-plane magnetic hysteresis at 10 K.

300 K in either 0 T or 0.2 T. A gradual transition is observed in the 120 K vicinity and agrees well with the temperature dependency determined from the neutron diffraction peak in Fig. 2(b). The difference between the field-cooled and zero-field-cooled data shows the formation of irreversible magnetization concurrent with the transition to long-range antiferromagnetic order.

In previous work on $\text{BiMn}_{0.5}\text{Fe}_{0.5}\text{O}_3$, high cooling fields were found to affect the apparent magnetic transition temperature, and this was considered to be suggestive of spin-glass behavior.²² However, the neutron result shows that long-range antiferromagnetic order predominates at low temperature, making it necessary to consider an alternative explanation for this dependency. One possibility is that the spin reorientation to the antiferromagnetic state is similar to the Morin transition in $\alpha\text{-Fe}_2\text{O}_3$ in that the cooling field plays a role in overcoming the inherent exchange frustration of the competing antiferromagnetic and Dzyaloshinskii–Moriya exchange.²⁸

Fig. 2(d) is the magnetic hysteresis at 10 K. A non-saturating magnetic hysteresis is seen with a coercivity of 0.3 T and a magnetization which has a value of $\approx 20 \pm 3 \text{ emu/cm}^3$ at 1 T. In the event that Mn and Fe order on alternate B sites to form an ordered double perovskite, a theoretical study predicts antiferromagnetic exchange between two sublattices with unequal spin, leading to a magnetic moment of approximately $1 \mu_B$ per Mn-Fe pair.²⁷ This would cause a far larger volume magnetization at low fields ($\approx 100 \text{ emu/cm}^3$) than what we,²² and other groups, have observed experimentally ($\approx 5\text{--}20 \text{ emu/cm}^3$).^{23,25} Therefore, along with the absence of superlattice peaks in the neutron diffraction, the magnetometry provides strong evidence that Mn/Fe are highly disordered across B sites in the host crystal matrix, and the magnetic response is due to canted antiferromagnetism as in the case for similar compounds hematite $\alpha\text{-Fe}_2\text{O}_3$ ²⁹ and BiFeO_3 . The non-rectangular shape of the hysteresis is typical for a canted antiferromagnetic material.³⁰ The magnetic response for the sample fits the trend identified by Yang *et al.* who studied $\text{BiMn}_x\text{Fe}_{1-x}\text{O}_3$ on SrTiO_3 with $x = 0.65, 0.75, 0.82, 0.9$ and found, for all cases, a magnetic transition below 120 K, with a systematic increase of magnetic moment with x where the magnetization was $\approx 15 \text{ emu/cm}^3$ for $x = 0.65$ for $H = 0.1 \text{ T}$ at 10 K.²³ The result also matches the work of Bi *et al.* who studied epitaxial $\text{BiMn}_{0.5}\text{Fe}_{0.5}\text{O}_3$ thin films on SrTiO_3 (001) and found a near-zero magnetization (0.8 emu/cm^3) at room temperature and a ten-fold enhancement for $\text{BiMn}_{0.5}\text{Fe}_{0.5}\text{O}_3$ at 5 K (6 emu/cm^3 at 1 T),²⁵ although in the current work, higher measurement fields (5 T) were applied to avoid measuring the minor hysteresis loop. On the other hand, Choi *et al.* reported a remarkably high magnetic saturation (110 emu/cm^3) at room temperature and low fields for epitaxial $\text{BiMn}_{0.5}\text{Fe}_{0.5}\text{O}_3$ on SrTiO_3 (001) consistent with strain-induced ferromagnetism in the 300 Å films.²⁴ A full thickness dependency of $\text{BiMn}_{0.5}\text{Fe}_{0.5}\text{O}_3$ thin films has yet to be published but may reconcile both sets of experimental findings, since strain could be expected to alter significantly the nature of the Mn-O-Mn super-exchange.¹³ In previous work, the magnetic order was inferred from volume-averaged magnetometry measurements, but neutron diffraction provides direct insight into the atomic-scale order in $\text{BiMn}_{0.5}\text{Fe}_{0.5}\text{O}_3$.

The existence of both antiferromagnetic order and magnetic hysteresis in $\text{BiMn}_{0.5}\text{Fe}_{0.5}\text{O}_3$ is evidence of the Dzyaloshinsky-Moriya interaction since this is the mechanism for canted antiferromagnetism.^{29,31,32} Second, this elicits the possibility of incommensurate cycloid features as for the case of BiFeO_3 which has a G-type antiferromagnetic order modulated by a long-wavelength spin spiral-cycloid. In thin films ($< 600 \text{ Å}$), the cycloid could not be detected in BiFeO_3 ³³ but recently a neutron diffraction study found clear signatures of this cycloid for thicker films ($1 \mu\text{m}$) on (110) and (111) SrTiO_3 .³⁴ To search for the appearance of incommensurate peaks, a 2D imaging of the $(\frac{1}{2}\frac{1}{2}\frac{1}{2})$ peak at 5 K was performed. Fig. 3 shows the $\text{BiMn}_{0.5}\text{Fe}_{0.5}\text{O}_3$ reciprocal space map in the $(\frac{1}{2}\frac{1}{2}\frac{1}{2})$ vicinity. For BiFeO_3 , a satellite reflection of almost equal intensity is found near $(\frac{1}{2}\frac{1}{2}\frac{1}{2})$ and is the main signature of the incommensurate spin cycloid. The dotted circles in Fig. 3 denote the approximate position in reciprocal space where the distinctive signature of $[\bar{\delta}\bar{\delta}2\delta]$ incommensurate peak would be apparent.³⁴ The absence of satellite features or non-ellipsoidal peak asymmetry near the main Bragg peak indicates that a cycloid was not detected for the $\text{BiMn}_{0.5}\text{Fe}_{0.5}\text{O}_3$ film despite the fact that the thin film shared the pseudo-cubic structure and G-type AF order with the parent BiFeO_3 compound. The absence of a cycloid in $\text{BiMn}_{0.5}\text{Fe}_{0.5}\text{O}_3$ may be advantageous for multiferroic properties, since the incommensurate structure is considered to be highly disadvantageous in BiFeO_3 where it lowers the magnetic saturation and prevents the linear magnetoelectric effect.² Although the precise influence of the (001) SrTiO_3 substrate is not yet clear, the lack of a measurable cycloid is in line with a recent first principles calculation that studied the weakening of the Dzyaloshinsky-Moriya energy interaction in $\text{BiMn}_{0.5}\text{Fe}_{0.5}\text{O}_3$, and argued that this should result in a suppressed spin-cycloid to make this material a better candidate for electric field manipulation of magnetization.³⁵ This seems to be a feasible explanation, although there is the small possibility that the cycloid is longer in wavelength, has a significantly different propagation vector, or exists in a multi-domain state,³⁴ and therefore could not be detected in

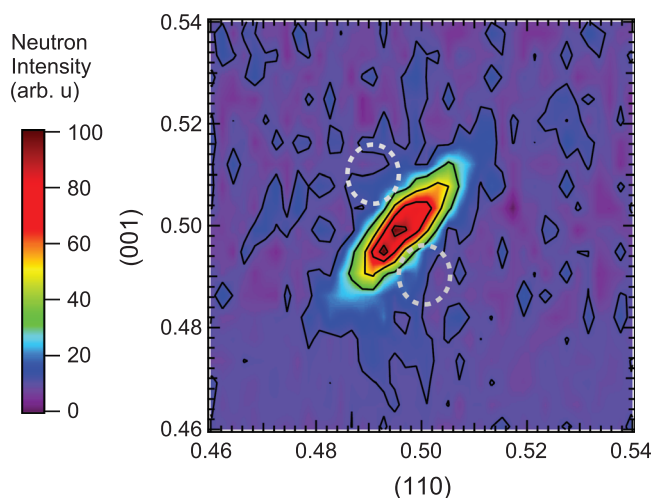


FIG. 3. Contour plot of reflected neutron intensity in the (110)/(001) scattering plane near the $(\frac{1}{2}\frac{1}{2}\frac{1}{2})$ position at 5 K. The absence of substructure and satellite reflections near the primary reflection indicates that the spin cycloid known for BiFeO_3 does not occur for $\text{BiMn}_{0.5}\text{Fe}_{0.5}\text{O}_3$ on SrTiO_3 (100).

the measurement. This is unlikely given the consensus with bulk $\text{BiMn}_x\text{Fe}_{1-x}\text{O}_3$ and $\text{La}_y\text{Bi}_{1-y}\text{Mn}_{0.5}\text{Fe}_{0.5}\text{O}_3$ where no incommensurate features were reported,^{16,21} and due to the fact that the saturation magnetization in $\text{BiMn}_{0.5}\text{Fe}_{0.5}\text{O}_3$ appears to be enhanced relative to BiFeO_3 which is consistent with a suppressed cycloid.

In conclusion, this work has shown unambiguously that G-type antiferromagnetism exists in a 5900 Å-thick epitaxial $\text{BiMn}_{0.5}\text{Fe}_{0.5}\text{O}_3$ film below 120 K. We find that Mn and Fe are disordered across B sites such that ferrimagnetism cannot be realized. The spin cycloid known for BiFeO_3 could not be detected for $\text{BiMn}_{0.5}\text{Fe}_{0.5}\text{O}_3$ on SrTiO_3 (001). The magnetization of the $\text{BiMn}_{0.5}\text{Fe}_{0.5}\text{O}_3$ is increased with respect to BiFeO_3 but the transition temperature is reduced. Future work is needed to understand how the magnetic structure of this compound depends on film thickness and strain.

D.L.C. acknowledges the support of the Australian Institute Nuclear Science and Engineering.

¹N. Spaldin and M. Fiebig, *Science* **309**, 391 (2005).

²G. Catalan and J. F. Scott, *Adv. Mater.* **21**, 2463 (2009).

³M. Gajek, M. Bibes, S. Fusil, K. Bouzehouane, J. Fontcuberta, A. Barthélémy, and A. Fert, *Nature Mater.* **6**, 296 (2007).

⁴W. Eerenstein, N. D. Mathur, and J. F. Scott, *Nature* **442**, 759 (2006).

⁵H. Béa, M. Gajek, M. Bibes, and A. Barthélémy, *J. Phys.: Condens. Matter* **20**, 434221 (2008).

⁶S. M. Wu, S. Cybart, P. Yu, M. D. Russell, J. X. Zhang, R. Ramesh, and R. C. Dynes, *Nature Mater.* **9**, 756 (2010).

⁷T. Kimura, S. Kawamoto, I. Yamada, M. Azuma, M. Takano, and Y. Tokura, *Phys. Rev. B* **67**, 180401 (2003).

⁸J. Wang, J. B. Neaton, H. Zheng, V. Nagarajan, S. B. Ogale, B. Liu, D. Viehland, V. Vaithyanathan, D. G. Schlom, U. V. Waghmare, N. A. Spaldin, K. M. Rabe, M. Wuttig, and R. Ramesh, *Science* **299**, 719 (2003).

⁹C. J. Fennie, *Phys. Rev. Lett.* **100**, 167203 (2008).

¹⁰D. Y. Wang, N. Y. Chan, R. K. Zheng, C. Kong, D. M. Lin, J. Y. Dai, H. L. W. Chan, and S. Li, *J. Appl. Phys.* **109**, 114105 (2011).

¹¹E. Montanari, G. Calestani, A. Migliori, M. Dapiaggi, F. Bolzoni, R. Cabassi, and E. Gilioli, *Chem. Mater.* **17**, 6457 (2005).

¹²A. A. Belik, K. Kodama, N. Igawa, S. Shamoto, K. Kosuda, and E. Takayama-Muromachi, *J. Am. Chem. Soc.* **132**, 8137 (2010).

¹³D. P. Kozlenko, A. A. Belik, S. E. Kichanov, I. Mirebeau, D. V. Sheptyakov, T. Strässle, O. L. Makarova, A. V. Belushkin, B. N. Savenko, and E. Takayama-Muromachi, *Phys. Rev. B* **82**, 014401 (2010).

¹⁴Z. X. Cheng, X. L. Wang, Y. Du, and S. X. Dou, *J. Phys. D: Appl. Phys.* **43**, 242001 (2010).

¹⁵J. Sahu and C. Rao, *Solid State Sci.* **9**, 950 (2007).

¹⁶I. Sosnowska, W. Schäfer, W. Kockelmann, K. Andersen, and I. Troyanchuk, *Appl. Phys. A* **74**, S1040 (2001).

¹⁷H. Zhao, H. Kimura, Q. Yao, Y. Du, Z. Cheng, and X. Wang, in *Ferroelectrics—Material Aspects*, edited by M. Lallart (InTech, Janeza Trdine, 2011), pp. 237–258.

¹⁸V. R. Palkar, D. C. Kundaliya, and S. K. Malik, *J. Appl. Phys.* **93**, 4337 (2003).

¹⁹M. Azuma, H. Kanda, A. A. Belik, Y. Shimakawa, and M. Takano, *J. Magn. Magn. Mater.* **310**, 1177 (2007).

²⁰H. Zhao, H. Kimura, Z. Cheng, X. L. Wang, K. Ozawa, and T. Nishida, *J. Appl. Phys.* **108**, 093903 (2010).

²¹C. A. Bridges, A. S. Sefat, E. A. Payzant, L. Cranswick, and M. P. Paranthaman, *J. Solid. State. Chem.* **184**, 830 (2011).

²²H. Zhao, H. Kimura, Z. Cheng, X. L. Wang, K. Ozawa, and T. Nishida, *Phys. Status Solidi (RRL)* **11**, 314 (2010).

²³C.-H. Yang, J. H. Song, H. J. Lee, S. Yoon, T. Y. Koo, and Y. H. Jeong, *Phys. Status Solidi B* **241**, 1453 (2004).

²⁴E.-M. Choi, S. Patnaik, E. Weal, S.-L. Sahonta, H. Wang, Z. Bi, J. Xiong, M. G. Blamire, Q. X. Jia, and J. L. MacManus-Driscoll, *Appl. Phys. Lett.* **98**, 012509 (2011).

²⁵L. Bi, A. R. Taussig, H.-S. Kim, L. Wang, G. F. Dionne, D. Bono, K. Persson, G. Ceder, and C. A. Ross, *Phys. Rev. B* **78**, 104106 (2008).

²⁶Y. Du, Z. X. Cheng, S. X. Dou, X. L. Wang, H. Y. Zhao, and H. Kimura, *Appl. Phys. Lett.* **97**, 122502 (2010).

²⁷H. Wang, H. Huang, and B. Wang, *Sci. Adv. Mater.* **2**, 184–189 (2010).

²⁸H. Chow and P. Feffer, *Phys. Rev. B* **10**, 243 (1974).

²⁹A. Morrish, *Canted Antiferromagnetism: Hematite* (World Scientific, Singapore, 1994).

³⁰R. N. Bhowmik and A. Saravanan, *J. Appl. Phys.* **107**, 053916 (2010).

³¹I. Dzyaloshinsky, *J. Phys. Chem. Solids* **4**, 241 (1958).

³²T. Moriya, *Phys. Rev.* **120**, 91 (1960).

³³H. Béa, M. Bibes, X.-H. Zhu, S. Fusil, K. Bouzehouane, S. Petit, J. Kriess, and A. Barthélémy, *Appl. Phys. Lett.* **93**, 072901 (2008).

³⁴W. Ratcliff II, D. Kan, W. Chen, S. Watson, S. Chi, R. Erwin, G. J. McIntyre, S. C. Capelli, and I. Takeuchi, *Adv. Funct. Mater.* **21**, 1567 (2011).

³⁵H.-J. Feng, *J. Magn. Magn. Mater.* **324**, 178 (2012).